OFDM Allocation Optimization for Crosstalk Mitigation in Multiple Free-Space Optical Interconnection Links

Dima Bykhovsky and Shlomi Arnon

***Abstract*—The growing demand for high interconnection speed in next-generation computers is driving the technology-shift for communication from the electronic to the optic domain. One of the favored interconnection technologies for this task is the free-space optical interconnect (FSOI). FSOI technology uses laser links between computer components and provides a lower bound on propagation delay due to the low index of refraction of air, when compared with the indices common in waveguide technologies. FSOIs based on DC-biased optical orthogonal frequency-division multiplexing (DCO-OFDM) may provide excellent data throughput in intensity modulation/direct detection (IM/DD) systems. However, the main drawback limiting the implementation of FSOIs is the inevitable trade-off between interconnection density and the crosstalk level, resulting from the diffraction effect and from optical misalignment. The purpose of this paper is to promote improved interconnection density of such FSOIs by use of inherent DCO-OFDM resource allocation capabilities. The crosstalk-resulted interference was formulated as joint multi-link bit-and-power allocation optimization. The theoretical analysis reveals general guidelines for dense FSOI. Further, a reduced-complexity numerical sub-optimal algorithm for joint multi-link bit-and-power allocation was proposed. The simulation results show that the proposed suboptimal algorithm outcome is close to the theoretical optimal performance.**

***Index Terms*—discrete multitone modulation, DMT, OFDM, DCO-OFDM, FSOI, free-space optical interconnect, crosstalk, interference avoidance, multi-access communication, parallel optical interconnect**

I. Introduction

NEXT-generation computers will require ultra-high data-rates and low-latency interconnection links. The current communication solutions are based on multi-transceiver arrays interconnected by fiber ribbons. The recent implementations include numerous fiber-interconnected lasers and detectors organized as an array on a single chip. For example, Doany *et. al.* [1] implemented 48 transceivers in a 4×12 array chip and Benjamin [2] *et. al.* manufactured a chip with 168 transceivers. One of the promising next-step technologies for such links is the free-space optical interconnect (FSOI) [3]. FSOIs are the links in a technology for transmitting information without a waveguide, in which multiple beams propagate between the communicating components through free space (Fig. 1a).

D. Bykhovsky is with the Electro-optical Engineering Unit, Ben-Gurion University of the Negev, Beer-Sheva, Israel and with the Electrical and Electronics Engineering Department, Shamoon College of Engineering, Beer-Sheva, Israel.

S. Arnon is with the Electrical and Computer Engineering Department, Ben-Gurion University of the Negev, Beer-Sheva, Israel (e-mail: shlomi@ee.bgu.ac.il).

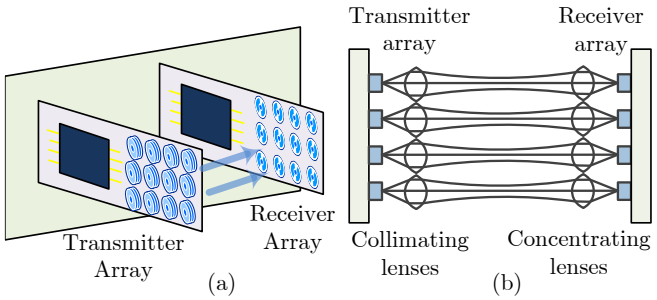

Fig. 1. (a) An example of a typical FSOI configuration that includes a 2D transceiver array [8], (b) a detailed illustration of the transceiver array, showing laser-based transmitters, each with a collimating lens and photodiode-based receivers, each with a concentrating lens [7].

FSOIs are a prominent subject of both past [3], [4], [5], [6], [7] and ongoing research [8], [9], [10], [11] due to their advantages over their waveguide counterpart. These include fewer physical contact points between the laser diode and the receiver, low weight and low propagation latency due to the low index of refraction of air, when compared with the indices common in waveguide technologies [3]. Moreover, sophisticated free-space switching may be applied for dynamic optical connections reconfiguration [5], [6], [8].

However, FSOIs are limited in interconnection distance, scalability and interconnection density, mainly due to the crosstalk and power degradation that typically result from axial misalignment and from the inevitable diffraction effect. The mentioned limitations of FSOI may be partially overcome in a number of ways. For example, the correction of axial misalignment can be achieved using active optical elements such as micro-electro-mechanical systems (MEMS) [8]. An additional approach applies wavelength reuse in order to provide denser interconnections [9]. Another simple tactic to reduce the optical crosstalk is to increase the separation between the transmitters/receivers in the transmitter/receiver array [12]. An alternative method for the mitigation of the crosstalk effect in multiple FSOI links uses advanced signal processing algorithms. Such algorithms include multiple-input multiple-output (MIMO)-based communication with [13], [14] or without [15] space-time coding (STC).

A further alternative that could mitigate these limitations, which is investigated in this paper, is to implement FSOI with orthogonal frequency-division multiplexing (OFDM)-based links. Intensity-modulation/direct-detection (IM/DD) DC-biased optical OFDM (DCO-OFDM) is favored for FSOI

because it displays excellent bit-rate performance and bandwidth utilization. It also enables significantly higher communication bit-rates than on-off keying (OOK) modulation [16], while employing a similar optical design. Lastly, OFDM exhibits the property of tuning flexibility that enables the mitigation of crosstalk by interference-coordinated bit-and-power allocation.

A. Main Contribution

This paper addresses the FSOI crosstalk problem in the context of DCO-OFDM resource allocation optimization. We address these two topics to propose a scheme that could provide fast and dense FSOIs. The main contribution of the paper is the proposed optimization of DCO-OFDM parameters to mitigate the crosstalk effect. We formulate the interference-affected FSOI communication scheme as a new optimization problem. The optimization addresses DCO-OFDM subcarrier allocation and the corresponding bit-and-power loading. The allocation guidelines are derived by theoretical analysis. Since the general optimal solution to such problems is computationally challenging, we suggest a lower-complexity sub-optimal algorithm for crosstalk mitigation by resource allocation.

B. Related Work

The optimization of OFDM resource allocation is a long-standing subject of interest in the field of cellular communication. Single-transmitter multi-user OFDM (MU-OFDM) schemes were devised, for example, by Rhee and Cioffi [17], Jang and Lee [18], Shen *et. al.* [19] and Kim *et. al.* [20]. The latter multi-transmitter MU-OFDM optimization method was revised by Rahman and Yanikomeroglu [21] and others.

For optical communication, the allocation optimization of single user [22] and MU [23], [24] OFDM optical links has already been formulated in the visible-light communication (VLC) context. Both [23] and [24] address the issue of resource allocation in dynamic optical networks. This paper modifies the resource allocation optimization described in [24] within the context of crosstalk-affected multiple FSOI links.

It is important to specify the main difference between the proposed design and the MIMO communication concept. A MIMO system requires persistent signal processing that is joint, simultaneous and time-synchronized for all spatially-diverse transmitters and receivers. In contrast, multiple OFDM point-to-point links require only transceiver clock synchronization and infrequent subcarrier and power allocation information that is sent to the transceivers via a separate control channel, as illustrated in Fig. 3.

The rest of the paper is organized as follows. Section II formulates crosstalk-impaired communication through FSOI links as the MU-OFDM resource allocation optimization problem and Section III shows an analytical approach to its solution. Section IV provides a description of the proposed sub-optimal optimization algorithm. Simulation results for the different communication scenarios are shown in Section V, followed by conclusions in Section VI.

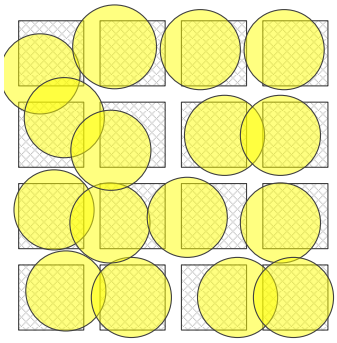

Fig. 2. An example of beam overlap in FSOI that is a result of beam deviation in a 4×4 two-dimensional (2D) receiver configuration.

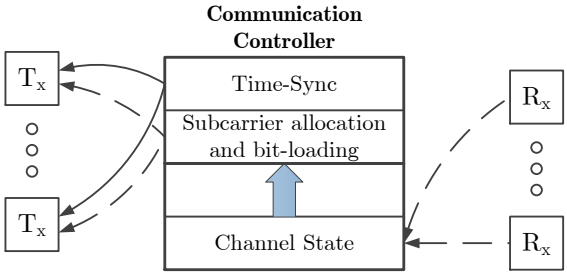

Fig. 3. OFDM communication can be implemented by almost independent (except for time-synchronization) point-to-point links with external resource management control, while the subcarrier and power allocation information is sent to the receivers via a separate control channel (T_x- transmitters, R_x - receivers).

II. Problem Formulation

A typical FSOI design includes a one- or two-dimensional (1D or 2D) array of laser-based transmitters and photodiode-based receivers, as presented in Fig. 1(b). The light beams of such a laser array may deviate from the center of the corresponding receiver detectors due to production defects, axial misalignment, mechanical impact and thermal expansion. Moreover, such deviation is influenced by the optical diffraction effect. As a result, beams overlap on more than one detector in the array and produce multiple crosstalk effects, as depicted in Fig. 2. In this section, the bit-rate analysis of crosstalk-affected FSOI is presented and the maximization of bit-rate is formulated as a resource allocation optimization problem.

A. Bit-Rate Formulation

The bit-rate analysis is based on the formula that describes the bound on bit error rate (BER) that is given by [25, Eq. (4.3-30)]

$$P_e \leqslant 4Q\left(\sqrt{\frac{3}{M-1}\mathrm{SINR}}\right), \tag{1}$$

where $Q(x)$ is the Q-function, $M = 2^b$ is the modulation order of an M-QAM scheme and SINR is the subcarrier signal-to-noise-and-interference ratio. From (1), the bit-rate as a function of SINR is given by

$$b \cong \log_2\left(1 + \frac{\mathrm{SINR}}{\Gamma}\right), \tag{2}$$

where $\Gamma = \left[Q^{-1}\left(P_e/4\right)\right]^2/3$ and P_e is the predefined uncorrected BER value. In the multiple interconnection environment, the electrical $\mathrm{SINR_{m,n}}$ at receiver m and for subcarrier n is given by [23], [24]

$$\mathrm{SINR}_{m,n} = \frac{p_{m,n}|h_{m,m,n}|^2}{\sum\limits_{\substack{k=1 \\ k\neq m}}^{K} p_{k,n}|h_{k,m,n}|^2 \ + p^{(n)}}, \tag{3}$$

where $p_{m,n}$ is the received electrical power, $h_{k,m,n}$ is the channel gain between the *k*th transmitter and the *m*th receiver at the *n*th subcarrier, K is the number of transceivers and the noise power, $p^{(n)} = N_0 B/N$, is a function of the noise power spectral density, N_0, signal bandwidth, B, and the number of subcarriers, N. The resulting total bit-rate at the *m*th receiver is given by

$$r_m = \sum_{n=1}^{N} b_{m,n} = \sum_{n=1}^{N} \log_2\left(1 + \frac{\mathrm{SINR}_{m,n}}{\Gamma}\right) \ . \tag{4}$$

The calculations above are based on the assumption of channel state information (CSI) being available both at the transmitter and at the receiver. Also, channels are assumed to be quasi-static, i.e. do not change within the time-span of a set of OFDM symbols [26], and are perfectly synchronized [27].

B. Optimization Formulation

Based on the total bit-rate expression above, the optimization formulation deals with bit-rate maximization in a crosstalk-resulted interference environment. The specific formulation depends on the particular link requirements as follows.

1) Max-sum bit-rate: The max-sum capacity allocation scheme aims to achieve the maximum bit-rate over all links together and is given by [18]

$$\max_{p,b} \sum_{m} r_m \ . \tag{5}$$

This allocation goal has inherent flexibility, since it does not require specific per link allocation.

2) Maximum equal bit-rate: The equal bit-rate optimization formulation requires that the communication bit-rate (4) is equal in all the links, regardless of the cross-influence of links on each other [1]. The allocation optimization is defined as the maximization of the overall bit rate of the multiple links

$$\max_{p,b} R_T, \tag{6}$$

where optimization is done over corresponding transmitter power values and

$$R_T = r_m \quad \forall m \tag{7}$$

is the requirement for equal bit-rate (4) in all links.

[1]In dynamic networks, this optimization corresponds to max-min (fair) allocation [17], [24].

3) Optimization Constraints: The optimization constraints are the same for all problem definitions above and are given by

$$\begin{aligned} \textstyle\sum_{n=1}^{N} p_{m,n} &\leqslant P_T && \forall m && \text{(8a)} \\ p_{m,n} &\geqslant 0 && \forall m,n && \text{(8b)} \\ b_{m,n} &\in 0,1,2,\ldots && \forall m,n\ , && \text{(8c)} \end{aligned}$$

where (8a) is the constraint on the maximum transmitter power P_T, (8b) requires non-negative allocated power $p_{m,n}$ and (8c) determines that the required target bit-rate $b_{m,n}$ at each transmitter and at each subcarrier (2) is a natural number (zero inclusive), since $2^{b_{m,n}}$ defines the QAM modulation order [2]. In the special case when $b_{m,n} = 1$, BPSK modulation can be used for the corresponding receiver-subcarrier pair.

The allocation solution involves nonlinear mixed integer optimization of a MN-dimensional integer variable $b_{m,n}$ and a continuous power variable $p_{m,n}$. Whenever subcarriers are organized in groups (chunks) of a few subcarriers (i.e. significantly reducing N) and for a low number of transceivers, M, the optimization problem can be addressed by mixed integer nonlinear programing (MINLP) solvers. However, the computation complexity of MINLP grows exponentially with the number of variables. Therefore, when this number grows beyond a few tens the numerical solution becomes computationally prohibitive.

III. Preliminary Analysis

In this section, we provide a preliminary analysis of different optimization aspects. This analysis is then applied to derive the numerical allocation algorithm in Section IV and to verify its performance in Section V.

A. Two-Step Optimization

In order to simplify the mixed-integer optimization outlined above, the problem may be reformulated as a two-step optimization [19]. First, the decision about subcarrier assignment is evaluated by the binary optimization of a new binary indicator variable $\rho_{m,n}$ [20], [21], [24] that is defined as

$$\rho_{m,n} = \begin{cases} 0, & b_{m,n} = 0 \\ 1, & \text{otherwise} \end{cases} \ , \tag{9}$$

where $\rho_{m,n} = 0$ means that the subcarrier n is restricted for use by the transceiver m. To simplify the allocation, the transmitted power, P_T, is equally divided among $\sum_{i=1}^{N} \rho_{m,i}$ active subcarriers. Therefore, the resulting modified $p_{m,n}$ expression is given by [26]

$$p_{m,n} = \rho_{m,n} \frac{P_T}{\sum_{i=1}^{N} \rho_{m,i}} \ . \tag{10}$$

Then, exact bit-and-power allocation is applied, based on the previously allocated subcarriers.

[2]Fractional/coded modulation is out of the scope of this paper.

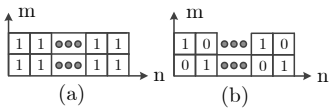

Fig. 4. The subcarrier states $\rho_{m,n}$ for (a) two interference ignorance links and (b) two interference avoidance links.

B. Interference Management Guidelines

Before proceeding to the allocation algorithm, some remarks are in order. Intuitively, one would assume that when the inter-channel crosstalk is low, the optimal optimization solution is *interference ignorance*, i.e. all subcarriers at all transceivers are used and $\rho_{m,n} = 1 \ \forall_{m,n}$ (Fig. 4(a)). Therefore, the performance of each channel is degraded in accordance with the crosstalk level experienced [24]. On the other hand, when the crosstalk is high, the subcarrier assignment is based on *interference avoidance*, i.e. only one channel is allowed to use each of the subcarriers. An example of subcarrier states that correspond to these situations (any combination of 50%/50% ones and zeros can be used) is presented in Fig. 4(b).

For example, for two channels with a frequency-flat channel gain of $h = 1$ and a symmetric cross-interference gain of h_i, the analytical bit-rate expression (4) is given by

$$r_m^{(i)} = N \log_2 \left(1 + \frac{1}{\Gamma} \frac{\gamma}{h_i^2 \gamma + N} \right) , \tag{11}$$

where $\gamma = P_T / p^{(n)}$ is the electrical signal SNR. This expression shows a successive bit-rate decrease as a function of the crosstalk value. The corresponding bit-rate expression for two links with the interference avoidance pattern is derived similarly, and is given by

$$r_m^{(a)} = \frac{N}{2} \log_2 \left(1 + \frac{2}{\Gamma} \frac{\gamma}{N} \right) . \tag{12}$$

The resulting bit-rate is about half the non-interfered bit-rate $r_m^{(i)}/2$ plus $N/2$ additional bits per QAM symbol that result from a $\times 2$ increase in the average power per subcarrier, since only half of the subcarriers are allocated. The resulting $r_m^{(a)}$ value is independent of the crosstalk (interference) level.

Generally, the bit-rate of a pure interference avoidance solution depends on the number of reuse solution patterns $\mathcal{R} \geqslant 2$. This number is defined as the minimum number of the required subcarrier reuse solutions $\rho_{m,n}$ that may be repeated cyclically for different subcarriers. For example, in Fig. 4(b) the reuse patterns are given by $\rho_m = (1\ 0)^T$ and $\rho_m = (0\ 1)^T$. Another example of a $\mathcal{R} = 2$ repetitive pattern is presented in Figs. 7b and 7c. An illustration depicting different $\mathcal{R}$ values for 2D transceiver arrays with different interference patterns is presented in Fig. 5. The corresponding bit-rate expression is derived similarly to above and is given by

$$r_m^{(a)} = \frac{N}{\mathcal{R}} \log_2 \left(1 + \frac{\mathcal{R}}{\Gamma} \frac{\gamma}{N} \right) . \tag{13}$$

The corresponded resultant bit-rate is about $1/\mathcal{R}$ times the non-interfered bit-rate plus $N/\mathcal{R} \log_2 \mathcal{R}$ additional bits per QAM symbol that result from a $\times \mathcal{R}$ increase in the average power per subcarrier.

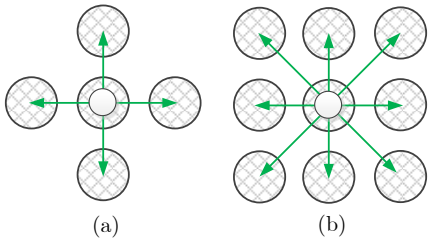

Fig. 5. Illustration of different interference examples. The general interference avoidance optimization $\rho_{m,n}$ requires (a) $\mathcal{R} = 2$ and (b) $\mathcal{R} = 4$ reuse patterns.

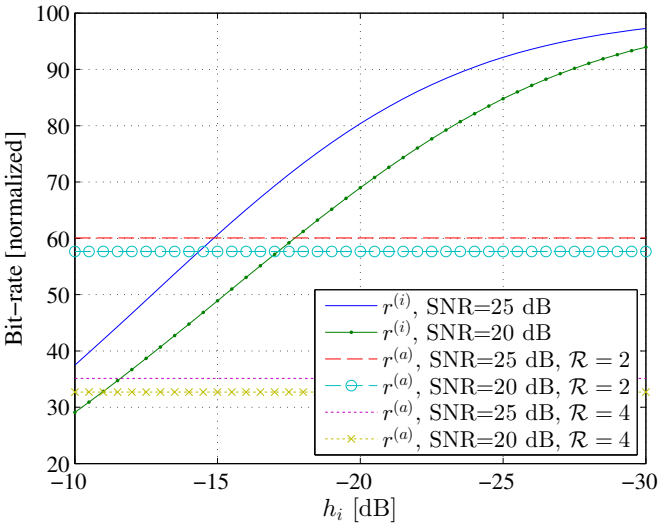

Fig. 6. The normalized interference ignorance and interference avoidance bit-rates ($r^{(i)}$ and $r^{(a)}$, correspondingly) for different reuse patterns (Fig. 5) and SNR levels as a function of crosstalk gain.

An illustration of this analysis for different $\mathcal{R}$ values is found in Fig. 6, where the bit-rate (y-axis) is normalized to the non-interfered link. It is clearly seen that there exists an interference threshold value, $h_i^{(thr)}$, such that whenever the interference is lower or higher than this value, i.e. $h_i \lessgtr h_i^{(thr)}$, the preferable interference management $r_m^{(i)} \gtrless r_m^{(a)}$ is selected correspondingly.

C. Optimization Formulation Guidelines

In order to illustrate the difference between the two different optimization problem definitions above, the following three-link example is presented (Fig. 7). Two links produce a significant crosstalk level between each other, i.e. $h_{i_1} > h_i^{(thr)}$, while other crosstalk values are significantly smaller, i.e. $h_{i_2} \ll h_i^{(thr)}$. The crosstalk-induced interference may be represented by a normalized channel gain matrix of the form

$$h_{k,m} = \begin{pmatrix} 1 & h_{i_1} & 0 \\ h_{i_1} & 1 & h_{i_2} \\ 0 & h_{i_2} & 1 \end{pmatrix} , \tag{14}$$

where h_{i_1} and h_{i_2} are interference gains.

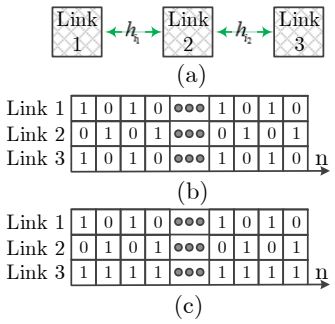

Fig. 7. Example of three-link configuration, where (a) each transceiver interferes with nearby links and allocation coefficients ($\rho_{m,n}$) are different for (b) maximum equal and (c) max-sum optimizations.

Whenever equal bit-rate optimization (6) is required, the optimal solution is interference avoidance for all three links, as shown in Fig. 7(b). The bit-rate of each link is given by

$$R_T = \frac{N}{2}\log_2\left(1+\frac{2}{\Gamma}\frac{\gamma}{N}\right) \tag{15}$$

and the total link bit-rate is $3R_T$.

When total bit-rate maximization (5) is required, the optimal solution is interference avoidance between "Link 1" and "Link 2" and interference ignorance at "Link 3". By substitution of the corresponding $\rho_{m,n}$ values, as shown in Fig. 7(c), the resulting bit-rates are given by

$$r_1 = \frac{N}{2}\log_2\left(1+\frac{2}{\Gamma}\frac{\gamma}{N}\right) \tag{16}$$

$$r_2 = \frac{N}{2}\log_2\left(1+\frac{2}{\Gamma}\frac{\gamma}{h_{i_2}^2\gamma+N}\right) \tag{17}$$

$$r_3 = \frac{N}{2}\log_2\left(1+\frac{1}{\Gamma}\frac{\gamma}{2h_{i_2}^2\gamma+N}\right) + \frac{N}{2}\log_2\left(1+\frac{1}{\Gamma}\frac{\gamma}{N}\right), \tag{18}$$

where r_1 in (16) is equal to r_T in (15), r_2 in (17) is similar to r_1, but the influence of the interference from "Link 3" and r_3 in (18) is influenced by "Link 2" in half of the subcarriers.

The difference between these two solutions is that bit-rate r_2 is slightly smaller than R_T, i.e. $r_2 \lessapprox R_T$, and bit-rate r_3 is slightly smaller than $2R_T$, i.e. $r_3 \lessapprox 2R_T$, following the results presented in Fig. 6. Finally, the total max-sum optimized bit-rate is bounded by $3R_T < \sum_m r_m \lessapprox 4R_T$, which is notably higher than for three links with an equal bit-rate of R_T each in the equal bit-rate optimization option. This discussion shows that the max-sum optimized interconnect has a significantly higher bit-rate and should be used whenever an equal bit-rate is not required.

IV. Proposed Solution

The proposed allocation solution comprises a two-step optimization, inspired by [19]. First, the decision about subcarrier assignment is evaluated by the binary optimization of the value of $\rho_{m,n}$, implemented by a greedy heuristic algorithm. Then, exact bit-and-power allocation of $b_{m,n}$ and $p_{m,n}$ is applied, based on the previously allocated subcarriers' assignment.

A. Max-Sum Bit-Rate Optimization

The subcarrier allocation can be achieved by a sub-optimal greedy heuristic algorithm that is inspired by the Hughes-Hartogs algorithm [28]. This incremental algorithm iteratively assigns one subcarrier at one transceiver at a time, while requiring the highest incremental bit-rate at the target BER. The allocation runs through all the subcarriers at all the transceivers. The essential algorithm flow is as follows:

1: **for** n from 1 to N **do**
2: **for** m from 1 to K **do**
3: $\rho^*_{m,n} = \rho_{m,n} + 1$
4: Evaluate r^*_m for $\rho^*_{m,n}$
5: **end for**
6: **if** $r_m < \max r^*_m$ **then**
7: $m^* = \arg\max_m \; r^*_m$
8: $\rho_{m^*,n} = \rho_{m^*,n} + 1$
9: **end if**
10: **end for**

Line 6 checks whether an additional increase in bit-rate is possible with the addition of a subcarrier. Finally, power allocation at each transmitter is evaluated independently by some common power allocation algorithm [26].

B. Equal Bit-rate Optimization

The proposed subcarrier allocation is done by the max-min approach, where the bit-rate is maximized for the link with the minimum assigned bit-rate. This allocation is carried out by the algorithm above, with the following change in line 6:

6: **if** $r_m < \min r^*_m$ **then**

The rest of the algorithm is the same. Since all bit-rates are equal, the power allocation is evaluated in order to comply with the bit-rate R_T (7) that is evaluated during the subcarrier allocation.

V. Simulation

A. Configuration

Transceivers are organized in arrays, where each link consists of a transmitter-receiver pair and experiences some crosstalk with neighboring links. The frequency response of each transmitter is modeled by a second-order low-pass filter with $N = 64$ subcarriers, where half of them are conjugate to the other half, due to the Hermitian symmetry requirement [29]. Power and crosstalk link parameters are taken from the work of Ciftcioglu *et. al.* [12]. The maximum link SNR at DC was set to 22.2 dB. The target BER bound P_e (1) was set to 10^{-3}, which leads to a final BER of $\sim 10^{-12}$ after applying forward-error-correction (FEC) coding [30]. The default crosstalk level between adjacent links is 23 dB, if not stated otherwise. The common bit-and-power allocation applied through the proposed algorithm is the original Hughes-Hartogs algorithm [28].

The analyzed scenario is based on a 4×4 link, as show in Fig. 2, when each transmitter may interfere with four adjacent links, as presented in Fig. 5(a). This interference may be either uniform or non-uniform, according to the specific scenario.

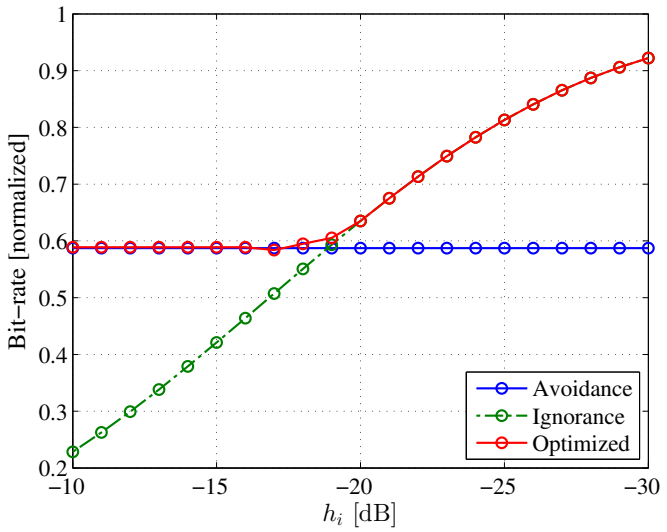

Fig. 8. Results of a preliminary simulation that show that an allocation algorithm produces a switch between numerical interference ignorance and analytical interference avoidance (12) solutions.

The performance is evaluated in terms of average bit-rate normalized by the bit-rate of a non-interfered link.

B. Preliminary Simulation

The goal of the preliminary simulation is to verify that the evaluated results comply with the theoretical findings above (Sec. III-B). The interference of each a link is symmetric, i.e. all adjacent links have the same interference channel gain h_i. The max-sum normalized bit-rate of such a link as a function of h_i is presented in Fig. 8. The graph shows that the optimized bit-rate (y-axis) behavior is in accordance with the theoretical analysis, while the switch between the numerical interference ignorance ($\rho_{m,n} = 1$) and the analytical interference avoidance (12) solutions is clearly seen at the h_i of about -19 dB.

C. Simulation Results

The next scenario is based on the situation where the interference is $h_i = -23$ dB and one of the transmitters produces an excessive interference channel gain of $h_{i2} = -12$ dB for four adjacent links, as presented in Fig. 9(a).

The result of the max-sum allocation is presented in Fig. 9(b) (the disk area in the figure is relative to the bit-rate) and shows that the link that produces the maximum interference has the lowest bit-rate. In contrast, the corner links have the highest allocated bit-rate since they produce and experience the lowest interference.

Following this scenario, the results of maximum equal bit-rate allocation were evaluated and presented in Fig. 9(c). The results show that the most interfered links require the highest power and the corner links have the lowest allocated power since they experience the lowest interference. The normalized bit-rate R_T is significantly lower than in max-sum optimization (0.67 for max-sum versus $R_T = 0.39$), as predicted by the theoretical analysis (Sec. III-C). However, the total power is 58% (-3.7 dB) less than in max-sum optimization, due to the reduction of the required power at a low-interfered link (Fig. 9(c)).

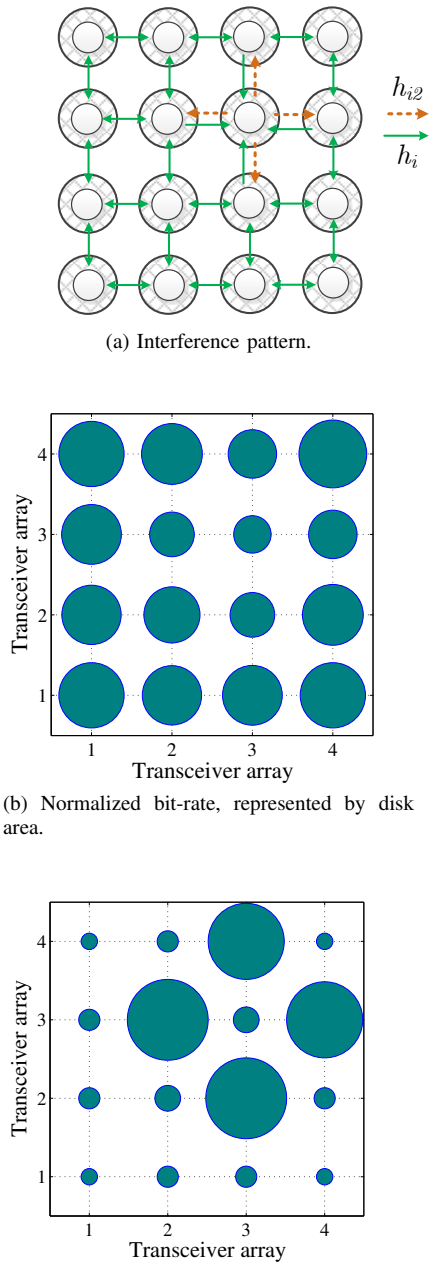

(a) Interference pattern.

(b) Normalized bit-rate, represented by disk area.

(c) Normalized power, represented by disk area.

Fig. 9. Scenario studied in the simulation in Section V-C. The inner and outer circles in (a) represent transmitter-receiver pairs. The sizes of the dots in (b) and (c) indicate bit-rate allocation for max-sum optimization and power allocation for equal bit-rate optimization, correspondingly.

D. Discussion

The results show that max-sum optimization is preferable in order to maximize the total bit-rate performance of dense FSOI, when compared to the equal bit-rate optimization in all links. The reason is that whenever some link experiences excessive interference, it becomes a bottleneck. On the other hand, in max-sum optimization the most interfering links are assigned the lowest bit-rate so that the neighbor links are less affected by the interference.

VI. Conclusions

An FSOI design comprises 2D arrays of transceivers, where each link may suffer from crosstalk from any other transceiver. The exact crosstalk level may be unknown during the manufacturing process, although some typical values are expected. This paper suggests a new FSOI communication concept and proposes an optimization algorithm to reduce the crosstalk effect computationally, rather than by changes in optical design.

The proposed algorithm addresses the mitigation of crosstalk effects by means of the optimization of signal modulation. Multiple DCO-OFDM modulated links are managed by means of bit-and-power allocation to maximize the bit-rate of a crosstalk-corrupted FSOI. The preliminary analysis revealed an intuitive allocation strategy that was devolved into a two-stage allocation algorithm. The simulation study showed that this algorithm displays flexibility in responding to different crosstalk levels and that the crosstalk-related decrease in the bit-rate is reasonable in the considered scenarios. Such flexibility also enables an adaptation in the bit-rate with a constant BER and power that is unavailable in OOK communication.

References

[1] F. Doany, B. Lee, D. Kuchta, A. Rylyakov, C. Baks, C. Jahnes, F. Libsch, and C. Schow, "Terabit/sec VCSEL-based 48-channel optical module based on Holey CMOS transceiver IC," *Journal of Lightwave Technology*, vol. 31, no. 4, pp. 672–680, Feb 2013.

[2] S. Benjamin, K. Hasharoni, A. Maman, S. Stepanov, M. Mesh, H. Luesebrink, R. Steffek, W. Pleyer, and C. Stommer, "336-channel electro-optical interconnect: Underfill process improvement, fiber bundle and reliability results," in *IEEE 64th Electronic Components and Technology Conference (ECTC)*, May 2014, pp. 1021–1027.

[3] L. J. Camp, R. Sharma, and M. R. Feldman, "Guided-wave and free-space optical interconnects for parallel-processing systems: a comparison," *Appl. Opt.*, vol. 33, no. 26, pp. 6168–6180, Sep 1994.

[4] S. Tang, R. T. Chen, D. J. Gerold, M. M. Li, C. Zhao, S. Natarajan, and J. Lin, "Design limitations of highly parallel free-space optical interconnects based on arrays of vertical-cavity surface-emitting laser diodes, microlenses, and photodetectors," in *Proc. SPIE*, ser. Optoelectronic Interconnects II, vol. 2153, no. 323, May 1994, pp. 323–333.

[5] E. Dietrich, H. Ehlers, M. Ferstl, B. Kuhlow, H. Kobolla, E. Pawlowski, G. Przyrembel, T. Rosin, G. Teich, J. Vathke, and G. Walf, "Free space interconnection system with holographic optical elements," in *Proceedings of 20th European Conference on Optical Communication (ECOC)*, Firenze, Italy, Sep. 1994, pp. 293–296.

[6] B. Kuhlow, G. Teich, and G. Walf, "OFDM cross-connect with an embedded free-space switch," in *Photonics in Switching*, vol. 12, Salt Lake City, Utah, Mar. 1995, pp. 24–26.

[7] A. G. Kirk, D. V. Plant, M. H. Ayliffe, M. Chateauneuf, and F. Lacroix, "Design rules for highly parallel free-space optical interconnects," *IEEE Journal of Selected Topics in Quantum Electronics*, vol. 9, no. 2, pp. 531–547, 2003.

[8] K. Wang, A. Nirmalathas, C. Lim, E. Skafidas, and K. Alameh, "Experimental demonstration of high-speed free-space reconfigurable card-to-card optical interconnects," *Optics Express*, vol. 21, no. 3, pp. 2850–2861, Feb 2013.

[9] D. Bykhovsky and S. Arnon, "Design and simulation of optical unguided bus interconnect," *IEEE Photonics Technology Letters*, vol. 24, no. 15, pp. 1353–1355, Aug. 2012.

[10] W. Hu, X. Li, J. Yang, and D. Kong, "Crosstalk analysis of aligned and misaligned free-space optical interconnect systems," *Journal of the Optical Society of America A*, vol. 27, no. 2, pp. 200–205, Feb 2010.

[11] N. Al-Ababneh and A. Al Jumah, "Analytical models for channel crosstalk in short-range free space optical interconnects," *Optical Engineering*, vol. 51, no. 11, pp. 115 401–1–6, 2012.

[12] B. Ciftcioglu, R. Berman, S. Wang, J. Hu, I. Savidis, M. Jain, D. Moore, M. Huang, E. G. Friedman, G. Wicks, and H. Wu, "3-D integrated heterogeneous intra-chip free-space optical interconnect," *Optics Express*, vol. 20, no. 4, pp. 4331–4345, Feb. 2012.

[13] S. V. Chinta, T. P. Kurzweg, D. S. Pfeil, and K. R. Dandekar, "4×4 space-time codes for free-space optical interconnects," in *Photonics Packaging, Integration, and Interconnects IX*, 2009, vol. 7221, pp. 722 116–8.

[14] D. Bykhovsky and S. Arnon, "Unguided optical communication 2×2 MIMO bus implementation," *IEEE Photonics Technology Letters*, vol. 23, no. 21, pp. 1597 –1599, Nov. 2011.

[15] D. O'Brien, "Optical multi-input multi-output systems for short-range free-space data transmission," in *7th International Symposium on Communication Systems Networks and Digital Signal Processing (CSNDSP)*, 2010, pp. 517–521.

[16] D. J. F. Barros, S. K. Wilson, and J. M. Kahn, "Comparison of orthogonal frequency-division multiplexing and pulse-amplitude modulation in indoor optical wireless links," *IEEE Transactions on Communications*, vol. 60, no. 1, pp. 153–163, Jan 2012.

[17] W. Rhee and J. Cioffi, "Increase in capacity of multiuser OFDM system using dynamic subchannel allocation," in *IEEE 51st Vehicular Technology Conference Proceedings*, vol. 2, 2000, pp. 1085–1089.

[18] J. Jang and K.-B. Lee, "Transmit power adaptation for multiuser OFDM systems," *IEEE Journal on Selected Areas in Communications*, vol. 21, no. 2, pp. 171–178, 2003.

[19] Z. Shen, J. Andrews, and B. Evans, "Adaptive resource allocation in multiuser OFDM systems with proportional rate constraints," *IEEE Transactions on Wireless Communications*, vol. 4, no. 6, pp. 2726–2737, 2005.

[20] I. Kim, I.-S. Park, and Y. H. Lee, "Use of linear programming for dynamic subcarrier and bit allocation in multiuser OFDM," *IEEE Transactions on Vehicular Technology*, vol. 55, no. 4, pp. 1195–1207, 2006.

[21] M. Rahman and H. Yanikomeroglu, "Enhancing cell-edge performance: a downlink dynamic interference avoidance scheme with inter-cell coordination," *IEEE Transactions on Wireless Communications*, vol. 9, no. 4, pp. 1414–1425, 2010.

[22] J. Grubor and K.-D. Langer, "Efficient signal processing in OFDM-based indoor optical wireless links," *Journal of Networks*, vol. 5, no. 2, Feb 2010.

[23] B. Ghimire and H. Haas, "Self-organising interference coordination in optical wireless networks," *EURASIP Journal on Wireless Communications and Networking*, vol. 2012, no. 1, p. 131, 2012.

[24] D. Bykhovsky and S. Arnon, "Multiple access resource allocation in visible light communication systems," *Journal of Lightwave Technology*, vol. 32, no. 8, pp. 1594–1600, 2014.

[25] J. G. Proakis and M. Salehi, *Digital Communications*, 5th ed. McGraw-Hill, 2008.

[26] D. Bykhovsky and S. Arnon, "An experimental comparison of different bit-and-power-loading algorithms for DCO-OFDM," *Journal of Lightwave Technology*, vol. 32, pp. 1559–1564, 2014.

[27] S. Arnon, "The effect of clock jitter in visible light communication applications," *Journal of Lightwave Technology*, vol. 30, no. 21, pp. 3434–3439, Nov 2012.

[28] D.Hughes-Hartogs, "Ensemble modem structure for imperfect transmission media," U.S. Patent 4,679,227, July 1987; 4,731,816, Mar. 1988; and 4,833,796, May 1989.

[29] J. Armstrong, "OFDM for optical communications," *Journal of Lightwave Technology*, vol. 27, no. 3, pp. 189–204, Feb. 2009.

[30] T. Mizuochi, Y. Miyata, T. Kobayashi, K. Ouchi, K. Kuno, K. Kubo, K. Shimizu, H. Tagami, H. Yoshida, H. Fujita, and et al., "Forward error correction based on block turbo code with 3-bit soft decision for 10-Gb/s optical communication systems," *IEEE Journal of Selected Topics in Quantum Electronics*, vol. 10, no. 2, pp. 376–386, Mar 2004.